Preprints of the 19th World Congress
The International Federation of Automatic Control
Cape Town, South Africa. August 24-29, 2014

Integral FCS Predictive Current Control of Induction Motor Drive

Liuping Wang* and Lu Gan*

* *School of Electrical and computer Engineering, RMIT University, Victoria 3000 Australia. e-mail: liuping.wang@rmit.edu.au*

Abstract: This paper derives the algorithm of integral plus finite control set (FCS) -predictive control for AC motor drives. In the paper, it is shown that the original FCS-predictive control algorithm in the $d-q$ reference frame is equivalent to a dead-beat control system in the presence of constraints, where the closed-loop system is approximated by a unit time delay. Without integral action, the original FCS-predictive control system contains steady-state errors in both d-axis and q-axis currents, hence compromising closed-loop performance. Using an integral control in a cascaded structure to the original FCS-predictive control, a simple algorithm is proposed to eliminate the steady-state errors of the current control system and improve its closed-loop performance. The sampling interval of the current control system is used as a performance tuning parameter for reduction of current variations. Furthermore, the algorithm is expressed in a velocity form for convenience in implementation using a digital signal processor. Experimental results are used to show the successful design and implementation of the integral finite control set (I-FCS) predictive control.

Keywords: AC-machine drives, predictive control, integral control, constrained control

1. INTRODUCTION

In last several years, the Finite Control Set (FCS)-predictive control arises in the research field of power electronics, due to its simple concept and robust performance. One of the early works of FCS was presented in Rodriguez et al. [2007], which compared FCS-predictive control with other control techniques, such as Pulse-Width-Modulation (PWM) and hysteresis. With PWM based implementation, the similar control method of deadbeat control was developed in earlier literature (Kukrer [1996]). Similar control techniques have also been published with different applications, such as Permanent Magnet Synchronous Motor (Moon et al. [2003], Morel et al. [2009], Preindl and Bolognani [2013]) and power converters (Vargas et al. [2007], Perez et al. [2011], Lezana et al. [2009], Vargas et al. [2009]). More recently, the FCS-MPC algorithms have been reviewed in Rodriguez and Cortes [2012] and Rodriguez et al. [2013]. Furthermore, there are several research questions associated the FCS-MPC methods developed, such as weighting factor calculation, uncertain switching frequency and steady-state error. The steady-state error issue is caused because the original FCS-MPC methods are optimization based without incorporating an integrator. To counteract this issue, Aguilera et al. [2013] presents approaches of intermediate sampling and integral error term in the cost function with application of a simple H-Bridge power converter. Another approach of embedding an on-line adaptation in the control system is studied in Ahmed et al. [2011] for LCL Coupled Inverter-Based Distributed Generation Systems. Moreover, Perez et al. [2011] presents the reduction of steady-state error for the predictive control of the dc-link voltage in an active-front-end rectifier.

In this paper, with the same objective to eliminate the steady-state error, the original FCS method is analysed and revised to become a feedback control system designed using one-step-ahead prediction and optimization. Within this framework, FCS-predictive control system is shown to have eigenvalues on the origin of the complex plane without the constraints. When constraints are introduced the errors between the optimal control signals and the constrained control signals are treated as input disturbance errors that has zero mean. Upon modelling the original FCS predictive control system as a single delay, an integrator is used in the outer-loop controller to effectively eliminate the steady-state errors.

2. ANALYSIS OF ORIGINAL FCS-PREDICTIVE CONTROL ALGORITHM

The continuous-time model that describes the dynamics of an induction motor in dq coordinates are given by the differential equations:

$$\frac{di_{sd}}{dt} = -\frac{1}{\tau'_\sigma} i_{sd} + \omega_s i_{sq} + \frac{k_r}{r_\sigma \tau'_\sigma \tau_r}\psi_{rd} + \frac{1}{r_\sigma \tau'_\sigma} u_{sd} \quad (1)$$

$$\frac{di_{sq}}{dt} = -\omega_s i_{sd} - \frac{1}{\tau'_\sigma} i_{sq} - \frac{k_r}{r_\sigma \tau'_\sigma}\omega\psi_{rd} + \frac{1}{r_\sigma \tau'_\sigma} u_{sq} \quad (2)$$

where the model constants $\sigma = 1 - \frac{L_h^2}{L_s L_r}$, $\tau_r = \frac{L_r}{R_r}$, $k_r = \frac{L_h}{L_r}$, $r_\sigma = R_s + R_r k_r^2$ and $\tau'_\sigma = \frac{\sigma L_s}{r_\sigma}$ are derived from the machine parameters.

From (1) and (2), it can be easily verified that the system matrices $A_m(t)$ and B_m are written in the following forms:

$$A_m(t) = \begin{bmatrix} -\dfrac{1}{\tau_\sigma} & \omega_s(t) \\ -\omega_s(t) & -\dfrac{1}{\tau_\sigma} \end{bmatrix};\; B_m = \begin{bmatrix} \dfrac{1}{\tau_\sigma r_\sigma} & 0 \\ 0 & \dfrac{1}{\tau_\sigma r_\sigma} \end{bmatrix}$$

The difference equations corresponding to (1) and (2) are

$$x(t_i + \Delta t) = (I + \Delta t A_m(t_i))x(t_i) + \Delta t B_m u(t_i) + \Delta t \gamma_D(t_i) \tag{3}$$

where $x(t_i) = [i_{sd}(t_i)\ i_{sq}(t_i)]^T$, $u(t_i) = [u_{sd}(t_i)\ u_{sq}(t_i)]^T$, $\gamma_D(t_i) = [\frac{k_r}{r_\sigma \tau_r \tau'_\sigma}\psi_{rd}(t_i)\ \ -\frac{k_r}{r_\sigma \tau'_\sigma}\omega(t_i)\psi_{rd}(t_i)]^T$ and I is the identity matrix with dimension 2×2.

2.1 Optimal Control System

In order to analyze the closed-loop performance via feedback control, the objective function J is re-written in vector form:

$$J = \begin{bmatrix} i^*_{sd}(t_i) - i_{sd}(t_i + \Delta t) \\ i^*_{sq}(t_i) - i_{sq}(t_i + \Delta t) \end{bmatrix}^T \begin{bmatrix} i^*_{sd}(t_i) - i_{sd}(t_i + \Delta t) \\ i^*_{sq}(t_i) - i_{sq}(t_i + \Delta t) \end{bmatrix} \tag{4}$$

For notational simplicity, let the vector $[\, f_d(t_i)\ \ f_q(t_i)\,]^T$ be defined as

$$\begin{bmatrix} f_d(t_i) \\ f_q(t_i) \end{bmatrix} = \begin{bmatrix} i^*_{sd}(t_i) \\ i^*_{sq}(t_i) \end{bmatrix} - (I + \Delta t A_m(t_i)) \begin{bmatrix} i_{sd}(t_i) \\ i_{sq}(t_i) \end{bmatrix} - \Delta t \gamma_D(t_i) \tag{5}$$

Then it can be verified by combining (5) with (3) that the objective function (4) has the compact expression:

$$J = \left(\begin{bmatrix} f_d(t_i) \\ f_q(t_i) \end{bmatrix} - \Delta t B_m \begin{bmatrix} u_{sd}(t_i) \\ u_{sq}(t_i) \end{bmatrix} \right)^T \left(\begin{bmatrix} f_d(t_i) \\ f_q(t_i) \end{bmatrix} - \Delta t B_m \begin{bmatrix} u_{sd}(t_i) \\ u_{sq}(t_i) \end{bmatrix} \right) \tag{6}$$

which is in the quadratic objective function form:

$$J = [\, f_d(t_i)\ \ f_q(t_i)\,] \begin{bmatrix} f_d(t_i) \\ f_q(t_i) \end{bmatrix} - 2\,[\, u_{sd}(t_i)\ \ u_{sq}(t_i)\,]\, \Delta t B_m^T \begin{bmatrix} f_d(t_i) \\ f_q(t_i) \end{bmatrix} + [\, u_{sd}(t_i)\ \ u_{sq}(t_i)\,]\, \Delta t^2 B_m^T B_m \begin{bmatrix} u_{sd}(t_i) \\ u_{sq}(t_i) \end{bmatrix} \tag{7}$$

From the quadratic objective function (7), by adding and subtracting the term

$$[\, f_d(t_i)\ \ f_q(t_i)\,]\, \Delta t B_m (\Delta t^2 B_m^T B_m)^{-1} B_m^T \Delta t \begin{bmatrix} f_d(t_i) \\ f_q(t_i) \end{bmatrix}$$

to the original objective function J, its value remains unchanged. With this term added, the following three terms lead to completed squares:

$$\begin{aligned} J_0 = {} & [\, u_{sd}(t_i)\ \ u_{sq}(t_i)\,]\, \Delta t^2 B_m^T B_m \begin{bmatrix} u_{sd}(t_i) \\ u_{sq}(t_i) \end{bmatrix} \\ & - 2\,[\, u_{sd}(t_i)\ \ u_{sq}(t_i)\,]\, \Delta t B_m^T \begin{bmatrix} f_d(t_i) \\ f_q(t_i) \end{bmatrix} \\ & + [\, f_d(t_i)\ \ f_q(t_i)\,]\, \Delta t B_m (\Delta t^2 B_m^T B_m)^{-1} B_m^T \Delta t \begin{bmatrix} f_d(t_i) \\ f_q(t_i) \end{bmatrix} \end{aligned}$$

which is

$$\begin{aligned} J_0 = {} & \left(\begin{bmatrix} u_{sd}(t_i) \\ u_{sq}(t_i) \end{bmatrix} - (\Delta t^2 B_m^T B_m)^{-1} B_m^T \Delta t \begin{bmatrix} f_d(t_i) \\ f_q(t_i) \end{bmatrix} \right)^T \\ & \times (\Delta t^2 B_m^T B_m) \\ & \times \left(\begin{bmatrix} u_{sd}(t_i) \\ u_{sq}(t_i) \end{bmatrix} - (\Delta t^2 B_m^T B_m)^{-1} B_m^T \Delta t \begin{bmatrix} f_d(t_i) \\ f_q(t_i) \end{bmatrix} \right) \end{aligned} \tag{8}$$

Equation (8) can be easily verified by opening the squares. Now, with J_0 given by the completed squares (8), the original objective function J becomes

$$J = J_0 + J_{min} \tag{9}$$

where J_{min} is

$$\begin{aligned} J_{min} = {} & -[\, f_d(t_i)\ \ f_q(t_i)\,]\, B_m (B_m^T B_m)^{-1} B_m^T \begin{bmatrix} f_d(t_i) \\ f_q(t_i) \end{bmatrix} \\ & + [\, f_d(t_i)\ \ f_q(t_i)\,] \begin{bmatrix} f_d(t_i) \\ f_q(t_i) \end{bmatrix} \end{aligned}$$

Note that the weighting matrix $\Delta t^2 B_m^T B_m$ in J_0 (see (8)) is positive definite and J_{min} is independent of the variables $u_{sd}(t_i)$ and $u_{sq}(t_i)$. Thus, the minimum of the original objective function J is achieved if J_0 is minimized. Furthermore, it is seen that the minimum of J_0 is zero, from (8), if variables $u_{sd}(t_i)$ and $u_{sq}(t_i)$ are chosen to be

$$\begin{bmatrix} u_{sd}(t_i) \\ u_{sq}(t_i) \end{bmatrix} = (\Delta t^2 B_m^T B_m)^{-1} \Delta t B_m^T \begin{bmatrix} f_d(t_i) \\ f_q(t_i) \end{bmatrix} \tag{10}$$

With the completing squares approach, the constant term J_{min} can be easily examined via

$$J_{min} = [\, f_d(t_i)\ \ f_q(t_i)\,]\, (I - B_m (B_m^T B_m)^{-1} B_m^T) \begin{bmatrix} f_d(t_i) \\ f_q(t_i) \end{bmatrix}$$

Since

$$B_m = \begin{bmatrix} \dfrac{1}{r_\sigma \tau'_\sigma} & 0 \\ 0 & \dfrac{1}{r_\sigma \tau'_\sigma} \end{bmatrix}$$

it is easy to verify that the matrix $I - B_m(B_m^T B_m)^{-1} B_m^T$ is a zero matrix, which leads to $J_{min} = 0$, hence $J = J_0$ from (9). This is an interesting conclusion, which basically says that sum of squares error between the predicted and the reference signals is zero if the control signals are chosen according to (10).

2.2 Feedback Controller Gain

Observing (10), the feedback control gain in the one-step-ahead predictive control system at sampling instant t_i is

$$K_{fcs}(t_i) = \begin{bmatrix} \dfrac{r_\sigma \tau'_\sigma}{\Delta t} & 0 \\ 0 & \dfrac{r_\sigma \tau'_\sigma}{\Delta t} \end{bmatrix} (I + \Delta t A_m(t_i)) \tag{11}$$

which is obtained by examining the relationship between $[\, u_{sd}(t_i)\ u_{sq}(t_i)\,]^T$ and $[\, i_{sd}(t_i)\ i_{sq}(t_i)\,]^T$. Immediately, (11) reveals that the feedback controller gain K_{fcs} increases as the sampling interval Δt decreases. As $\Delta t \to 0$, the feedback controller gain $K_{fcs} \to \infty$. Furthermore, for some sufficiently small Δt, the controller gain could be approximated by

$$K_{fcs}(t_i) \approx \begin{bmatrix} \dfrac{r_\sigma \tau'_\sigma}{\Delta t} & 0 \\ 0 & \dfrac{r_\sigma \tau'_\sigma}{\Delta t} \end{bmatrix} \tag{12}$$

To determine the internal closed-loop stability of the one-step-ahead predictive control system, consider the discretized system model. By substituting the feedback control signal (10) into (3) where the reference signals are considered to be 0 in the original control law, it can be readily verified that the closed-loop system has the following form:

$$\begin{bmatrix} i_{sd}(t_i+\Delta t) \\ i_{sq}(t_i+\Delta t) \end{bmatrix} = \begin{bmatrix} 0 & 0 \\ 0 & 0 \end{bmatrix} \begin{bmatrix} i_{sd}(t_i) \\ i_{sq}(t_i) \end{bmatrix} \tag{13}$$

The two eigenvalues of the closed-loop system (13) are at the origin of the complex plane.

2.3 Constrained Optimal Control

The one-step-ahead prediction of the current control system presented is an optimal control system without constraints. However, the actuators to implement the control signals are limited to seven candidate sets of u_{sd} and u_{sq} combinations. In the induction motor control, the electrical angle $\theta_s(t)$ in the stator is used to generate these candidate voltage values. Here, $\theta_s(t)$ is computed using the following relationship:

$$\begin{aligned} \theta_s(t) &= \theta_e(t) + \frac{1}{\tau_r}\int_0^t \frac{i_{sq}(\tau)}{i_{sd}(\tau)} d\tau \\ &\approx \theta(t) + \frac{1}{\tau_r}\int_0^t \frac{i^*_{sq}(\tau)}{i^*_{sd}(\tau)} d\tau \end{aligned} \tag{14}$$

where $\theta_e(t)$ is the measured electrical rotor position from the encoder, and $i^*_{sd}(t)$ and $i^*_{sq}(t)$ are the current reference signals used to approximate the current feedback signals i_{sd} and i_{sq} because of their measurement noise. With $\theta_s(t_i)$ determined at the sampling time t_i, and V_{dc} being the voltage for the power supply, the seven pairs of candidate voltage variables are formed:

$$\begin{aligned}
&u^0_{sd} = 0;\quad u^1_{sd} = \frac{2}{3}V_{dc}cos\theta_s(t_i);\\
&u^0_{sq} = 0;\quad u^1_{sq} = -\frac{2}{3}V_{dc}sin\theta_s(t_i);\\
&u^2_{sd} = \frac{2}{3}V_{dc}cos(\theta_s(t_i) - \frac{2\pi}{3});\\
&u^2_{sq} = -\frac{2}{3}V_{dc}sin(\theta_s(t_i) - \frac{2\pi}{3});\\
&u^3_{sd} = \frac{2}{3}V_{dc}cos(\theta_s(t_i) - \frac{4\pi}{3});\\
&u^3_{sq} = -\frac{2}{3}V_{dc}sin(\theta_s(t_i) - \frac{4\pi}{3});\\
&u^4_{sd} = -\frac{2}{3}V_{dc}cos\theta_s(t_i);\; u^5_{sd} = -\frac{2}{3}V_{dc}cos(\theta_s(t_i) - \frac{2\pi}{3});\\
&u^4_{sq} = \frac{2}{3}V_{dc}sin\theta_s(t_i);\quad u^5_{sq} = \frac{2}{3}V_{dc}sin(\theta_s(t_i) - \frac{2\pi}{3});\\
&u^6_{sd} = -\frac{2}{3}V_{dc}cos(\theta_s(t_i) - \frac{4\pi}{3});\\
&u^6_{sq} = \frac{2}{3}V_{dc}sin(\theta_s(t_i) - \frac{4\pi}{3});
\end{aligned}$$

In the optimal control without constraints, the solution that minimizes the objective function is given by (10), which virtually leads to the zero value of the objective function J. Letting the optimal control signals be denoted by

$$\begin{bmatrix} u_{sd}(t_i)^{opt} \\ u_{sq}(t_i)^{opt} \end{bmatrix} = (\Delta t^2 B_m^T B_m)^{-1} B_m^T \Delta t \begin{bmatrix} f_d(t_i) \\ f_q(t_i) \end{bmatrix} \tag{15}$$

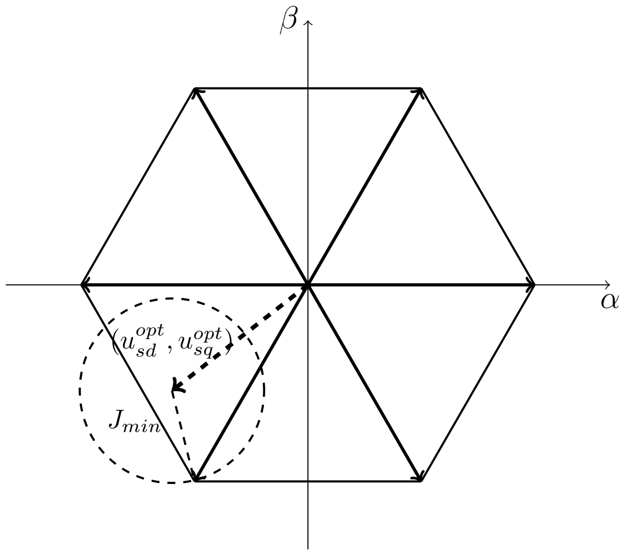

Fig. 1. Illustration of finite control set solution with $\theta = 0$

replacing the corresponding terms in the objective function J_0 with $\begin{bmatrix} u_{sd}(t_i)^{opt} & u_{sq}(t_i)^{opt} \end{bmatrix}^T$, we obtain the objective function for the constrained control problem:

$$\begin{aligned} J = &\left(\begin{bmatrix} u_{sd}(t_i) \\ u_{sq}(t_i) \end{bmatrix} - \begin{bmatrix} u_{sd}(t_i)^{opt} \\ u_{sq}(t_i)^{opt} \end{bmatrix} \right)^T (\Delta t^2 B_m^T B_m) \\ &\left(\begin{bmatrix} u_{sd}(t_i) \\ u_{sq}(t_i) \end{bmatrix} - \begin{bmatrix} u_{sd}(t_i)^{opt} \\ u_{sq}(t_i)^{opt} \end{bmatrix} \right) \end{aligned} \tag{16}$$

where $J = J_0$ because $J_{min} = 0$. Since the weighting matrix $\Delta t^2 B_m^T B_m$ is $\Delta t^2 B_m^T B_m$ is

$$\Delta t^2 B_m^T B_m = \begin{bmatrix} \frac{\Delta t^2}{L_\sigma^2} & 0 \\ 0 & \frac{\Delta t^2}{L_\sigma^2} \end{bmatrix}$$

where $L_\sigma = r_\sigma \tau'_\sigma$. the objective function J can also be written as

$$J = \frac{\Delta t^2}{L_\sigma^2}(u_{sd}(t_i) - u_{sd}(t_i)^{opt})^2 + \frac{\Delta t^2}{L_\sigma^2}(u_{sq}(t_i) - u_{sq}(t_i)^{opt})^2 \tag{17}$$

An immediate comment follows from (17). Note that the minimum value of the objective function when $u_{sd}(t_i) \neq u_{sd}(t_i)^{opt}$ and $u_{sq}(t_i) \neq u_{sq}(t_i)^{opt}$ is weighted by Δt^2, where Δt is the sampling interval. It is seen from (17) that the sampling interval Δt affects the minimum of the objective function J, hence, the variations of the d-axis and q-axis current signals.

To seek the optimal solution that will minimize the objective function J with the limited choices of $u_{sd}(t_i)$ and $u_{sq}(t_i)$, namely the seven pairs of $u_{sd}(t_i)$ and $u_{sq}(t_i)$, the seven values of the objective function J (17) are calculated with respect to the candidate pairs of $u_{sd}(t_i)$ and $u_{sq}(t_i)$ and denoted as $J^0, J^1, J^2, \ldots, J^7$. A simple search function is used to find the minimal value of J^m and its associated index.

There is a geometric interpretation for the minimization of the objective function (17) subject to the finite control set. The variations of the J form a family of circles centered at $(u_{sd}(t_i)^{opt}, u_{sq}(t_i)^{opt})$. The optimal solution is the pair of $u_{sd}(t_i)^k$ and $u_{sq}(t_i)^k$ values that touches the circle

in a shortest distance. This geometric interpretation is illustrated in Figure 1.
Although the original objective function (7) is identical to the objective function (17) after the analysis, the latter case offers an insight into the design problem, also more convenient in the computation of the control law. For the objective function (17), we can firstly calculate the feedback control gain K_{fcs} and the optimal control signal without constraints. Then we evaluate the cost function with the actual seven pairs of voltage variables against the optimal solution. The pair that yields a smallest cost function is the solution of the control signal.

3. INTEGRAL-FCS PREDICTIVE CONTROLLER

The derivation process in this section gives the justification of the algorithm and furthermore leads to the actual implementation algorithm for the I-FCS controller.

3.1 Integral-FCS Predictive Control Algorithm

Consider the discretized linear model for the induction motor (see (3)). This approximation of the continuous-time differential equation model also holds at the sampling time $t_i - \Delta t$, which has the form:

$$x(t_i) = (I + \Delta t A_m(t_i - \Delta t))x(t_i - \Delta t) + \Delta t B_m u(t_i - \Delta t) + \Delta t \gamma_D(t_i - \Delta t) \tag{18}$$

Subtracting (18) from (3) leads to the difference model between the two sampling instants:

$$\begin{aligned} x(t_i + \Delta t) - x(t_i) &= (I + \Delta t A_m(t_i))\,(x(t_i) - x(t_i - \Delta t)) \\ &+ \Delta t B_m(u(t_i) - u(t_i - \Delta t)) - \Delta t(\gamma_D(t_i) - \gamma_D(t_i - \Delta t)) \\ &+ \Delta t(A_m(t_i) - A_m(t_i - \Delta t))x(t_i - \Delta t) \end{aligned} \tag{19}$$

where in the process of derivation the following term is both added and subtracted to (19):

$$A_m(t_i)\Delta t \begin{bmatrix} i_{sd}(t_i - \Delta t) \\ i_{sq}(t_i - \Delta t) \end{bmatrix}$$

Note that matrix $(A_m(t_i) - A_m(t_i - \Delta t))\Delta t$ contained in the final term of (19) is expressed as

$$(A_m(t_i) - A_m(t_i - \Delta t))\Delta t = \begin{bmatrix} 0 & a_{12} \\ a_{21} & 0 \end{bmatrix}$$

where $a_{12} = -a_{21} = \Delta t(\omega_s(t_i) - \omega_s(t_i - \Delta t)$.
Because the quantity $\Delta t(\omega_s(t_i) - \omega_s(t_i - \Delta t)$ is sufficiently small for a small sampling interval Δt (say, 80×10^{-6} sec), the matrix $(A_m(t_i) - A_m(t_i - \Delta t))\Delta t$ is approximated by a zero matrix. Thus the final term of (19) is neglected. Approximation using zero for the second last term of (19) is also performed with the same reason.
The following incremental variables are defined for notational simplicity:

$$\Delta i_{sd}(t_i + \Delta t) = i_{sd}(t_i + \Delta t) - i_{sd}(t_i) \tag{20}$$
$$\Delta i_{sq}(t_i + \Delta t) = i_{sq}(t_i + \Delta t) - i_{sq}(t_i) \tag{21}$$
$$\Delta u_{sd}(t_i) = u_{sd}(t_i) - u_{sd}(t_i - \Delta t) \tag{22}$$
$$\Delta u_{sq}(t_i) = u_{sq}(t_i) - u_{sq}(t_i - \Delta t) \tag{23}$$

With these incremental variables defined and the approximations taken, the incremental model of an induction motor (19) becomes

$$\Delta x(t_i + \Delta t) = (I + \Delta t A_m(t_i))\Delta x(t_i) + \Delta t B_m \Delta u(t_i) \tag{24}$$

To include the integral action into the controller, we choose the weighted current errors $e_d(t_i) = k_I(i^*_{sd}(t_i) - i_{sd}(t_i))$ and $e_q(t_i) = k_I(i^*_{sq}(t_i) - i_{sq}(t_i))$ as the steady-states of the $\Delta i_{sd}(t_i)$ and $\Delta i_{sq}(t_i)$, where $0 < k_I < 1$. By subtracting the steady-states from the incremental model (24), it gives:

$$\begin{aligned} \begin{bmatrix} \Delta i_{sd}(t_i + \Delta t) - e_d(t_i) \\ \Delta i_{sq}(t_i + \Delta t) - e_q(t_i) \end{bmatrix} &= (I + \Delta t A_m(t_i)) \\ \begin{bmatrix} \Delta i_{sd}(t_i) - e_d(t_i) \\ \Delta i_{sq}(t_i) - e_q(t_i) \end{bmatrix} &+ \Delta t B_m \begin{bmatrix} \Delta u_{sd}(t_i) \\ \Delta u_{sq}(t_i) \end{bmatrix} \end{aligned} \tag{25}$$

The control objective is to minimize the error function J, where

$$J = \begin{bmatrix} \Delta i_d(t_i + \Delta t) - e_d(t_i) \\ \Delta i_q(t_i + \Delta t) - e_q(t_i) \end{bmatrix}^T \begin{bmatrix} \Delta i_d(t_i + \Delta t) - e_d(t_i) \\ \Delta i_q(t_i + \Delta t) - e_q(t_i) \end{bmatrix} \tag{26}$$

which is to regulate the incremental current signals $\Delta i_{sd}(t_i + \Delta t)$, $\Delta i_{sq}(t_i + \Delta t)$ to be as close as possible to $e_d(t_i)$ and $e_q(t_i)$.
For notational simplicity, define the vector:

$$\begin{aligned} \begin{bmatrix} g_d(t_i) \\ g_q(t_i) \end{bmatrix} &= -(I + \Delta t A_m(t_i)) \begin{bmatrix} \Delta i_d(t_i) - e_d(t_i) \\ \Delta i_q(t_i) - e_q(t_i) \end{bmatrix} \\ &= (I + \Delta t A_m(t_i)) \begin{bmatrix} e_d(t_i) - \Delta i_d(t_i) \\ e_q(t_i) - \Delta i_q(t_i) \end{bmatrix} \end{aligned} \tag{27}$$

Following the same procedure as outlined in Section 2 using the completing squares technique, the objective function (26) becomes

$$\begin{aligned} J = &\left(\begin{bmatrix} \Delta u_{sd}(t_i) \\ \Delta u_{sq}(t_i) \end{bmatrix} - (\Delta t^2 B_m^T B_m)^{-1} B_m^T \Delta t \begin{bmatrix} g_d(t_i) \\ g_q(t_i) \end{bmatrix} \right)^T \\ &\times (\Delta t^2 B_m^T B_m) \\ &\times \left(\begin{bmatrix} \Delta u_{sd}(t_i) \\ \Delta u_{sq}(t_i) \end{bmatrix} - (\Delta t^2 B_m^T B_m)^{-1} B_m^T \Delta t \begin{bmatrix} g_d(t_i) \\ g_q(t_i) \end{bmatrix} \right) \end{aligned} \tag{28}$$

This leads to the optimal solution of the incremental control signals without constraints:

$$\begin{bmatrix} \Delta u_{sd}(t_i)^{opt} \\ \Delta u_{sq}(t_i)^{opt} \end{bmatrix} = (\Delta t^2 B_m^T B_m)^{-1} B_m^T \Delta t \begin{bmatrix} g_d(t_i) \\ g_q(t_i) \end{bmatrix} \tag{29}$$

By substituting (29) into the objective function (26), we obtain

$$\begin{aligned} J = &\left(\begin{bmatrix} \Delta u_{sd}(t_i) \\ \Delta u_{sq}(t_i) \end{bmatrix} - \begin{bmatrix} \Delta u_{sd}(t_i)^{opt} \\ \Delta u_{sq}(t_i)^{opt} \end{bmatrix} \right)^T (\Delta t^2 B_m^T B_m) \\ &\left(\begin{bmatrix} \Delta u_{sd}(t_i) \\ \Delta u_{sq}(t_i) \end{bmatrix} - \begin{bmatrix} \Delta u_{sd}(t_i)^{opt} \\ \Delta u_{sq}(t_i)^{opt} \end{bmatrix} \right) \end{aligned}$$

Also, by definition of the incremental control signals, the following relationship is true:

$$\begin{bmatrix} \Delta u_{sd}(t_i)^{opt} \\ \Delta u_{sq}(t_i)^{opt} \end{bmatrix} = \begin{bmatrix} u_{sd}(t_i)^{opt} \\ u_{sq}(t_i)^{opt} \end{bmatrix} - \begin{bmatrix} \Delta u_{sd}(t_i - \Delta t)^{opt} \\ \Delta u_{sq}(t_i - \Delta t)^{opt} \end{bmatrix}$$

Thus, by calculating the actual incremental control signals using the same past control signal states, that is,

$$\begin{bmatrix} \Delta u_{sd}(t_i) \\ \Delta u_{sq}(t_i) \end{bmatrix} = \begin{bmatrix} u_{sd}(t_i) \\ u_{sq}(t_i) \end{bmatrix} - \begin{bmatrix} \Delta u_{sd}(t_i - \Delta t)^{opt} \\ \Delta u_{sq}(t_i - \Delta t)^{opt} \end{bmatrix}$$

Therefore, the objective function that can be used in the design of I-FCS is

$$J = \left(\begin{bmatrix} u_{sd}(t_i) \\ u_{sq}(t_i) \end{bmatrix} - \begin{bmatrix} u_{sd}(t_i)^{opt} \\ u_{sq}(t_i)^{opt} \end{bmatrix} \right)^T (\Delta t^2 B_m^T B_m)$$
$$\left(\begin{bmatrix} u_{sd}(t_i) \\ u_{sq}(t_i) \end{bmatrix} - \begin{bmatrix} u_{sd}(t_i)^{opt} \\ u_{sq}(t_i)^{opt} \end{bmatrix} \right)$$
$$= \frac{\Delta t^2}{L_\sigma^2}(u_{sd}(t_i) - u_{sd}(t_i)^{opt})^2 + \frac{\Delta t^2}{L_\sigma^2}(u_{sq}(t_i) - u_{sq}(t_i)^{opt})^2$$

In the presence of constraints, there are seven pairs of candidate variables for the u_{sd} and u_{sq} voltages. When having the integrators in the I-FCS controller, upon obtaining the signals $u_{sd}(t_i)^{opt}$ and $u_{sq}(t_i)^{opt}$ with integral action at the sampling time t_i, the actual control signals $u_{sd}(t_i)$ and $u_{sq}(t_i)$ are determined by computing the value of the objective function for $k = 0, 1, 2 \ldots, 6$

$$J^k = \frac{\Delta t^2}{L_\sigma^2}(u_{sd}(t_i)^k - u_{sd}(t_i)^{opt})^2 + \frac{\Delta t^2}{L_\sigma^2}(u_{sq}(t_i)^k - u_{sq}(t_i)^{opt})^2 \tag{30}$$

The pair of constrained control signals $u_{sd}(t_i)^k$ and $u_{sq}(t_i)^k$ is found to minimize the objective function J^k subject to the index number k.

3.2 Selection of Integral Control Gain

Figure 2 shows the cascade configuration of the I-FCS predictive control system, which is equivalent to the I-FCS predictive controller without constraints. The effect of the constraints is expressed in terms of a noise source that has zero mean. Because the closed-loop poles for the FCS predictive controller are at the origin of the complex plane, the inner-loop dynamics could be closely approximated by one sample of time delay as z^{-1}. Upon understanding the inner-loop system, the design of the outer-loop integral controller becomes straightforward. It is apparent that considering the d-axis current, the open-loop transfer function for the outer-loop system includes the integral controller $\frac{k_I}{1-z^{-1}}$ together with the time delay z^{-1} from the inner closed-loop system. Hence, the outer closed-loop has the transfer function:

$$\frac{I_{sd}(z)}{I_{sd}(z)^*} = \frac{k_I z^{-1}}{1 - z^{-1} + k_I z^{-1}} \tag{31}$$

where the closed-loop pole for this first order system is $1 - k_I$. By choosing a desired closed-loop pole as $0 \le P_{cl} < 1$, the integral controller gain is determined as $k_I = 1 - P_{cl}$.

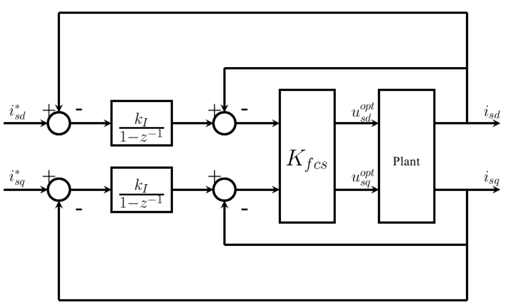

Fig. 2. Feedback current control using Integral FCS.

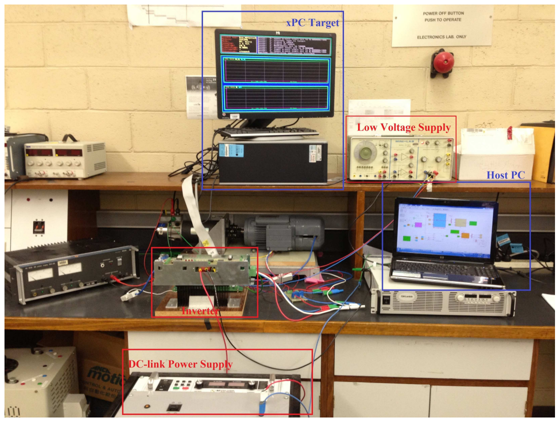

Fig. 3. Experimental test-bed of induction motor control.

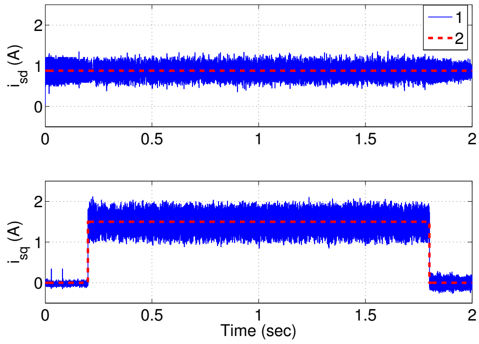

(a) Original FCS

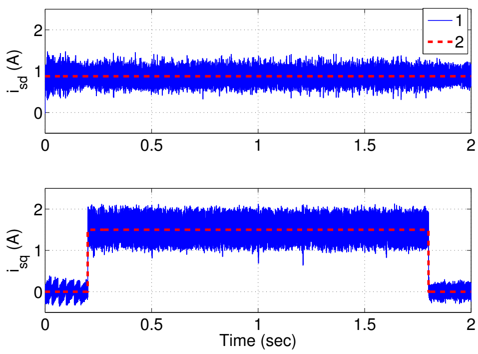

(b) Revised I-FCS

Fig. 4. Comparison with Experimental results of current control. Key: line(1): Actual measurement; line(2): Set-point signals.

4. EXPERIMENTAL RESULTS

The experiment results are obtained from a xPC Target-based induction motor control test-bed as shown in Figure 3. The MATLAB Simulink software is applied for control algorithm implementation and the induction motor is coupled with a servo DC motor as load. The supply voltage at DC-link is 520V.

The current set-points are $i_{sd}^* = 0.877$A and $i_{sq}^* = 1.5$A. The integral gain is designed as $k_I = 0.15$, the sampling time is $\Delta t = 80\mu$s.

Figure 4(b) shows the current control results of both $d-q$ axes. The results are satisfactory as the mean value of the

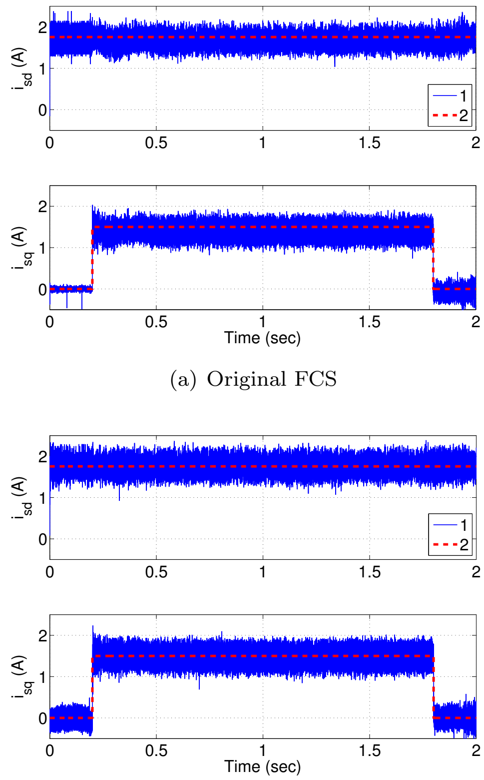

(a) Original FCS

(b) Revised I-FCS

Fig. 5. Comparison with Experimental results of current control with parameter mismatch. Key: line(1): Actual measurement; line(2): Set-point signals.

error $i^*_{sq} - i_{sq}$ is calculated to be -3.6636×10^{-4}. For comparison, Figure 4(a) presents the experimental results under exactly identical condition using the original FCS control method, where the mean value of the same error is 0.036. It is worthwhile to note that the steady-state response of the original FCS predictive control system is dependent on the selection of the system physical parameters. However, with the integral FCS predictive controller, this performance uncertainty in steady-state operation is removed.

To demonstrate this point, another set of comparison results is presented in Figure 5 with the parameter mismatching case, where the model parameter used for mutual inductance L_h was half of the original value. Under the identical experimental setting of the previous case, Figure 5(a) presents the experimental results of dq-axis current using original FCS method, the mean of steady-state error of i_{sq} current is increased to 0.0954, whereas the steady-state error mean using I-FCS is -8.6242×10^{-5} as shown in Figure 5(b). Based on the observation from Figure 5, the proposed I-FCS method presents its robustness in the parameter mismatching case, where the steady-state error was increased when applying the original FCS method.

5. CONCLUSION

This paper has proposed integral finite control set predictive control that will remove the steady-state errors in the original FCS predictive control system. An integral action is embedded in the FCS control design with cascaded structure using incremental model. The proposed control algorithm is validated using experimental results obtained from induction motor current control.

REFERENCES

R.P. Aguilera, P. Lezana, and D.E. Quevedo. Finite-control-set model predictive control with improved steady-state performance. *Industrial Informatics, IEEE Transactions on*, 9(2):658–667, 2013. ISSN 1551-3203.

K.H. Ahmed, A.M. Massoud, S.J. Finney, and B.W. Williams. A modified stationary reference frame-based predictive current control with zero steady-state error for lcl coupled inverter-based distributed generation systems. *Industrial Electronics, IEEE Transactions on*, 58 (4):1359–1370, 2011. ISSN 0278-0046.

O. Kukrer. Deadbeat control of a three-phase inverter with an output lc filter. *Power Electronics, IEEE Transactions on*, 11(1):16–23, 1996.

P. Lezana, R. Aguilera, and D.E. Quevedo. Model predictive control of an asymmetric flying capacitor converter. *Industrial Electronics, IEEE Transactions on*, 56(6): 1839–1846, 2009.

Hyung-Tae Moon, Hyun-Soo Kim, and Myung-Joong Youn. A discrete-time predictive current control for pmsm. *Power Electronics, IEEE Transactions on*, 18 (1):464–472, 2003.

F. Morel, Xuefang Lin-Shi, J.-M. Retif, B. Allard, and C. Buttay. A comparative study of predictive current control schemes for a permanent-magnet synchronous machine drive. *Industrial Electronics, IEEE Transactions on*, 56(7):2715–2728, 2009.

M.A. Perez, R.L. Fuentes, and J. Rodriguez. Predictive control of DC-link voltage in an active-front-end rectifier. In *Industrial Electronics (ISIE), 2011 IEEE International Symposium on*, pages 1811–1816, 2011.

M. Preindl and S. Bolognani. Model predictive direct speed control with finite control set of pmsm drive systems. *Power Electronics, IEEE Transactions on*, 28 (2):1007–1015, 2013.

J. Rodriguez and P. Cortes. *Predictive Control of Power Converters and Electrical Drives*. Wiley, 1st edition, 2012.

J. Rodriguez, J. Pontt, C.A. Silva, P. Correa, P. Lezana, P. Cortes, and U. Ammann. Predictive current control of a voltage source inverter. *Industrial Electronics, IEEE Transactions on*, 54(1):495–503, 2007.

J. Rodriguez, M.P. Kazmierkowski, J.R. Espinoza, P. Zanchetta, H. Abu-Rub, H.A. Young, and C.A. Rojas. State of the art of finite control set model predictive control in power electronics. *Industrial Informatics, IEEE Transactions on*, 9(2):1003–1016, 2013.

R. Vargas, P. Cortes, U. Ammann, J. Rodriguez, and J. Pontt. Predictive control of a three-phase neutral-point-clamped inverter. *Industrial Electronics, IEEE Transactions on*, 54(5):2697–2705, 2007.

R. Vargas, U. Ammann, and J. Rodriguez. Predictive approach to increase efficiency and reduce switching losses on matrix converters. *Power Electronics, IEEE Transactions on*, 24(4):894–902, 2009.